Electronic Supplementary Information （ESI）

Family of Lanthanide Metal-Organic Frameworks Based on Redox-Active Tetrathiafulvalene-Dicarboxylate Ligand Showing Slow Relaxation of Magnetisation and Electronic Conductivity

Jun-Jie Hu[a], Yu-Guang Li[a], He-Rui Wen*, [a], Sui-Jun Liu[a], Yan Peng[a] and Cai-Ming Liu*, [b]

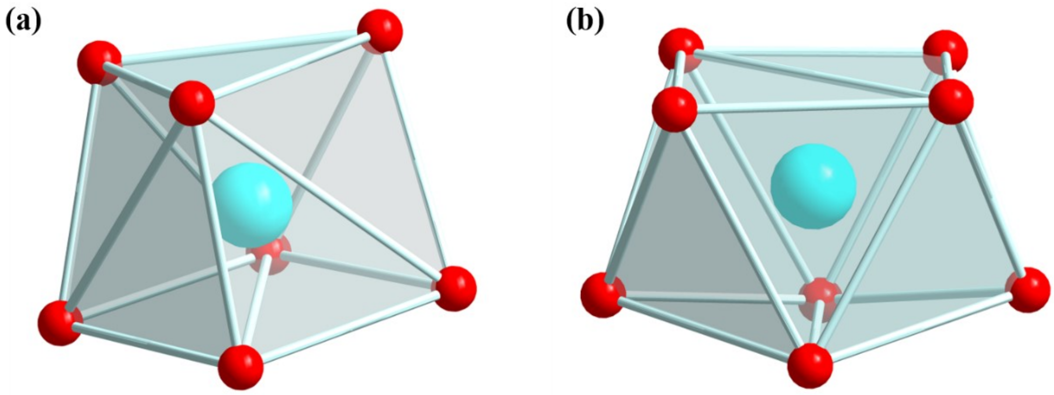

Figure S1. Coordination geometry around of Ln1 and Ln2 ions (a), Ln3 and Ln4 ions (b).

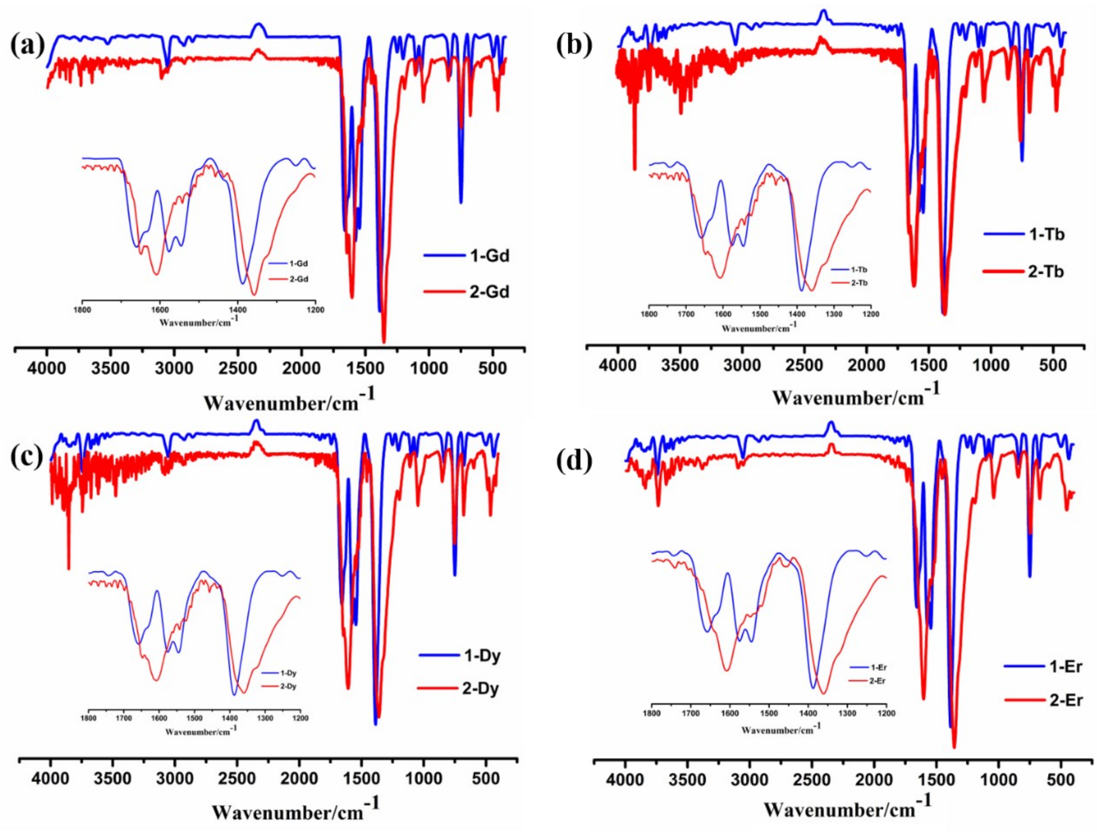

Figure S2. The IR spectra of **1-Ln** (a) and **2-Ln** (b).

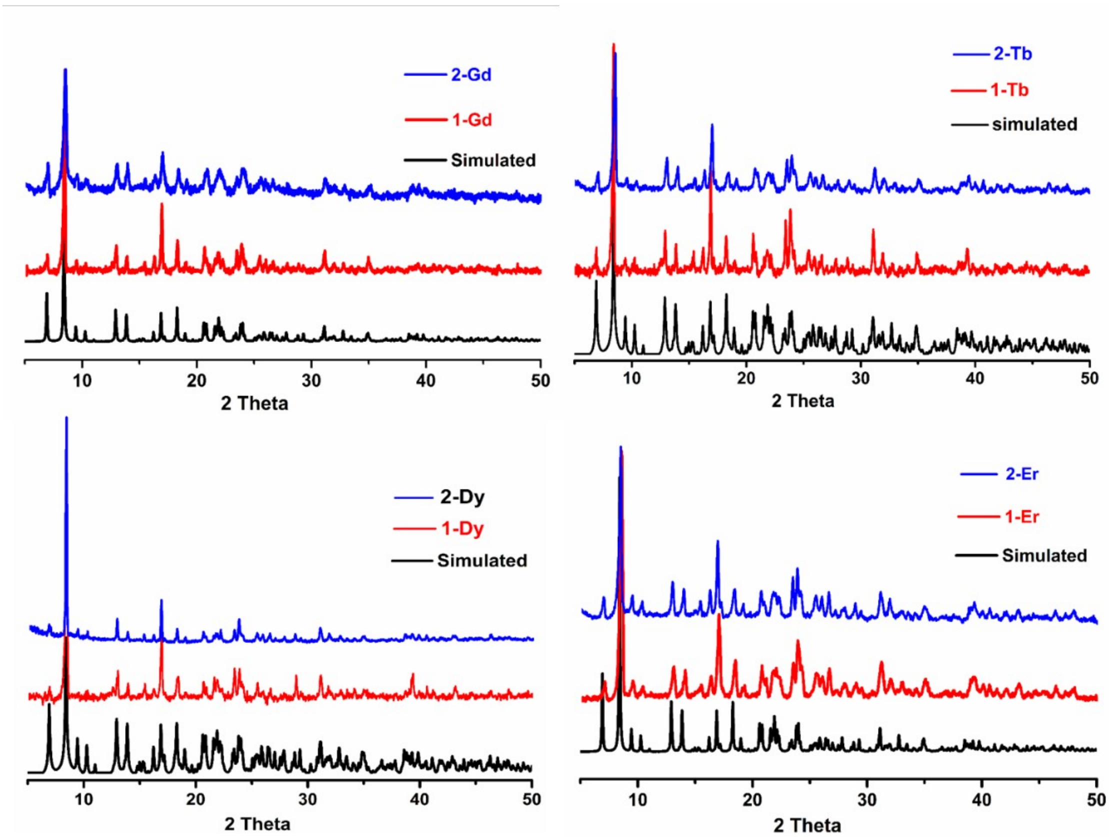

Figure S3. X-ray powder diffraction patterns of **1-Ln** and **2-Ln**.

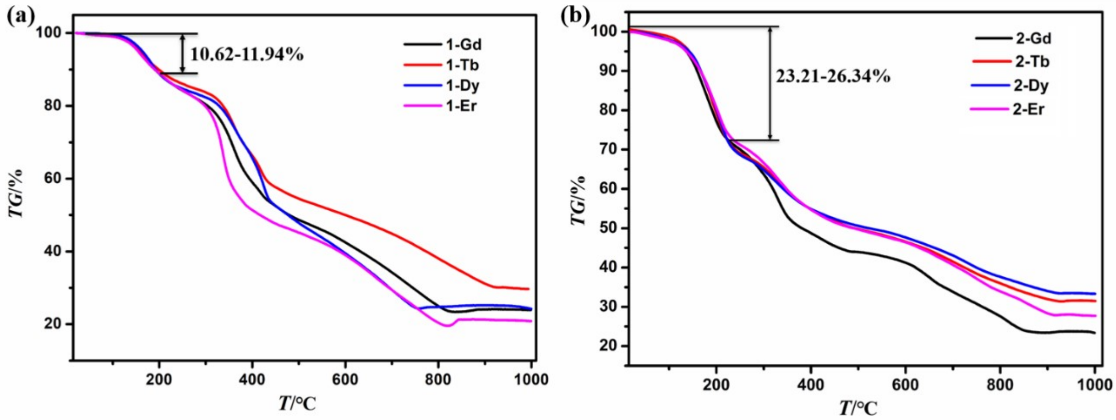

Figure S4. The TG plots of **1-Ln** (a) and **2-Ln** (b).

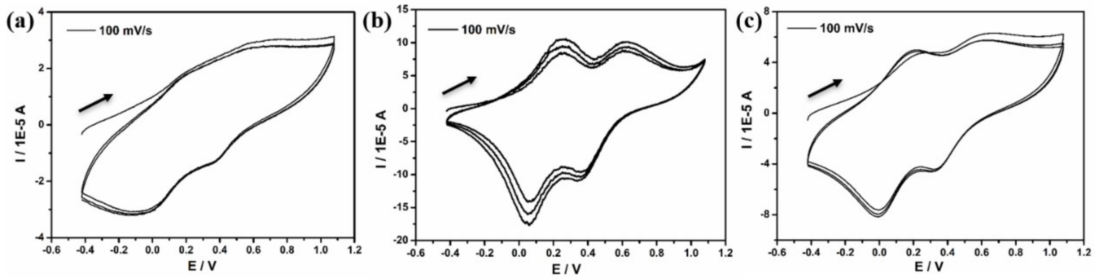

Figure S5. The cyclic voltammetry curve of crystal **1-Gd**，**1-Tb** and **1-Er** (vs. Fc/Fc^{+}) three forward scans. The arrow represents the scanning direction.

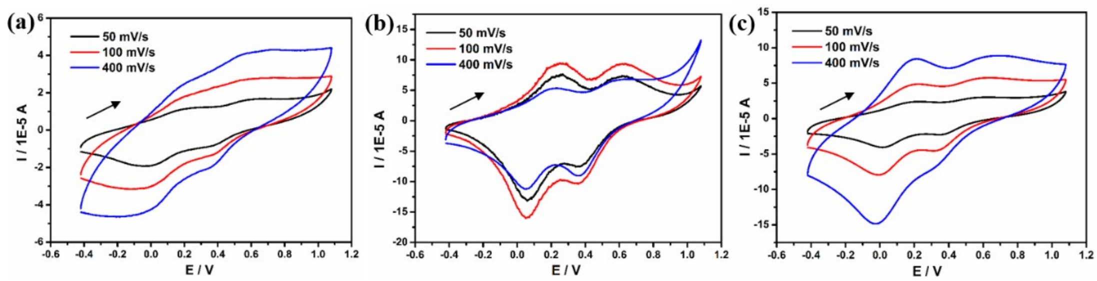

Figure S6. The cyclic voltammetry of crystal **1-Gd**，**1-Tb** and **1-Er** performed over different scan rates. The arrow represents the scanning direction.

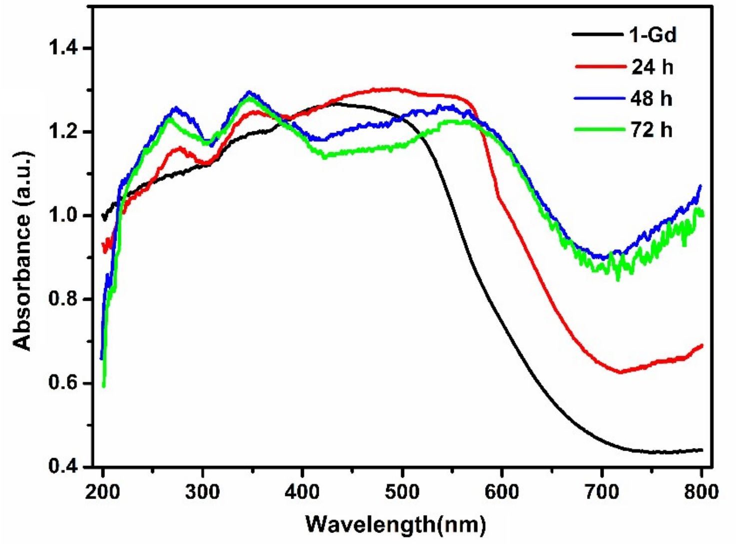

Figure S7. The solid-state UV/vis absorption spectra of **1-Gd** immersed in I_2 cyclohexane solution of iodine for different time.

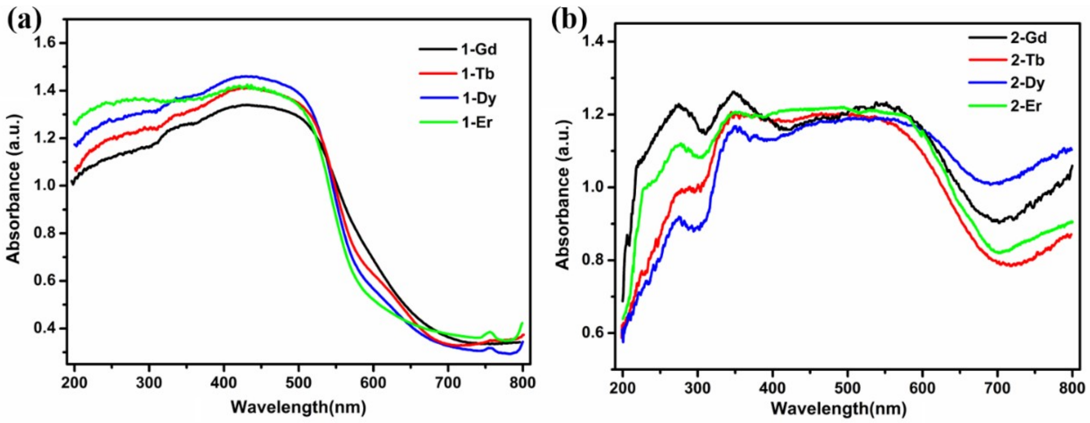

Figure S8. The solid-state UV/vis absorption spectrum of **1-Ln** (a) and **2-Ln** (b).

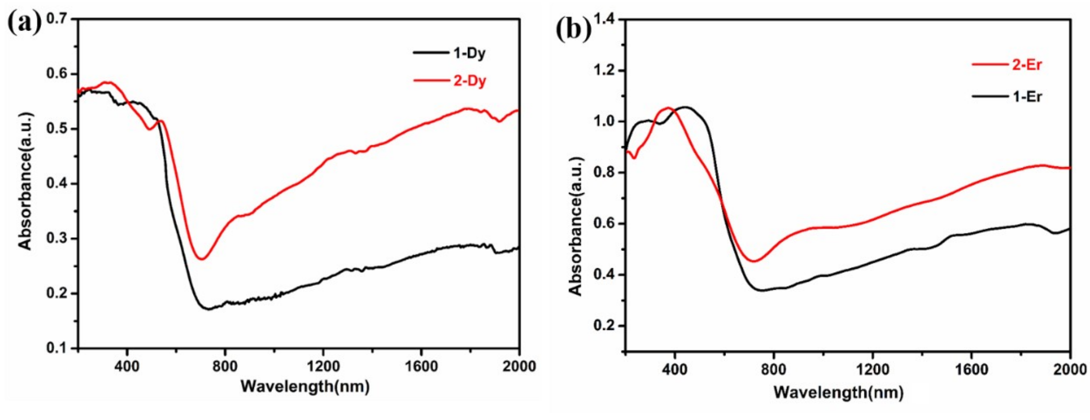

Figure S9. The solid-state UV-vis-NIR spectra of **1-Dy** and **2-Dy** (a), **1-Er** and **2-Er** (b).

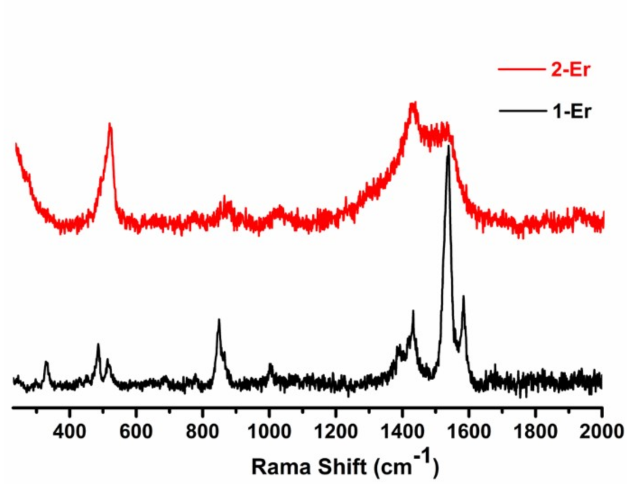

Figure S10. Raman spectra of **1-Er** and **2-Er**.

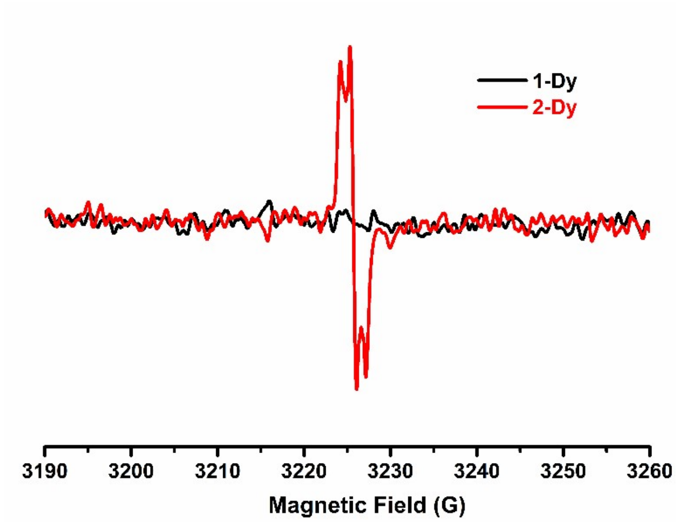

Figure S11. The Solid-state EPR spectra of **1-Dy** and **2-Dy** at room temperature.

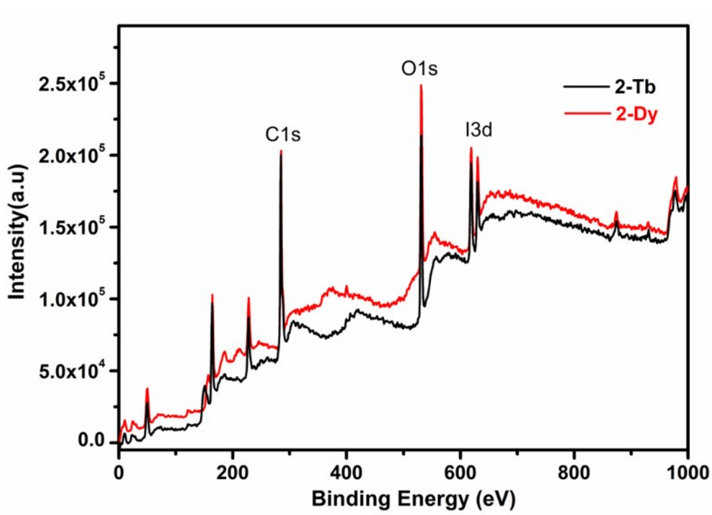

Figure S12. The XPS survey spectra of **2-Tb** and **2-Dy**.

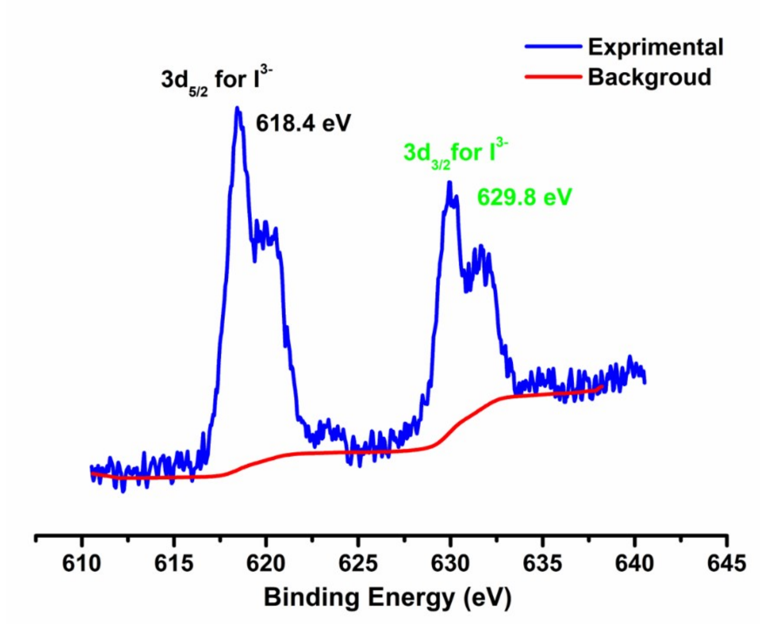

Figure S13. The XPS spectra for I3d with deconvolution of corresponding XPS peaks in **2-Tb**.

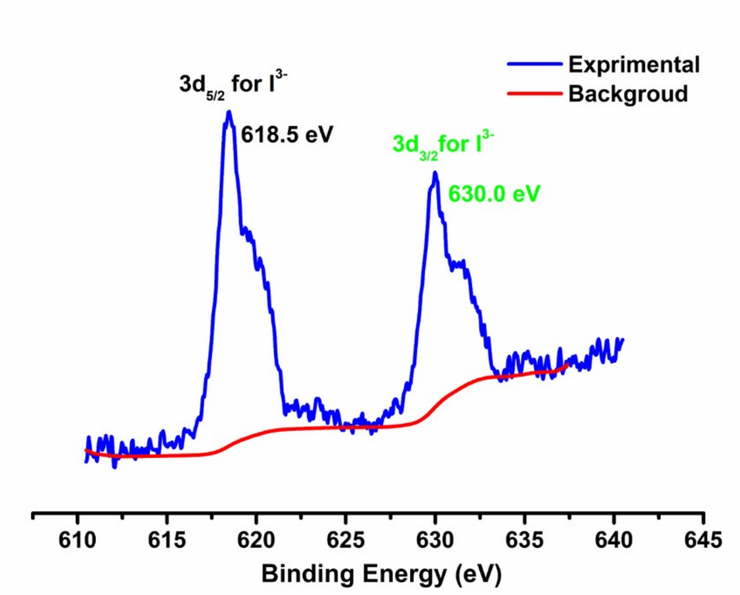

Figure S14. The XPS spectra for I3d with deconvolution of corresponding XPS peaks in **2-Dy**.

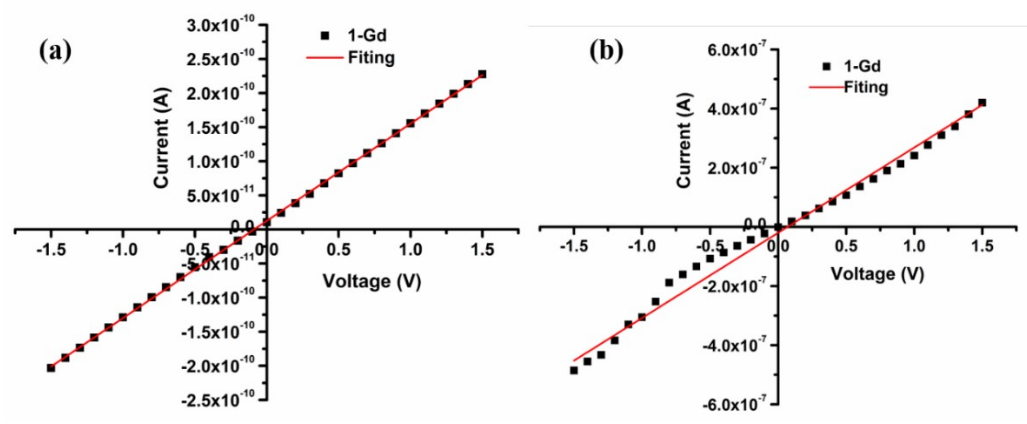

Figure S15. I-V curves of **1-Gd** (a) and **2-Gd** (b).

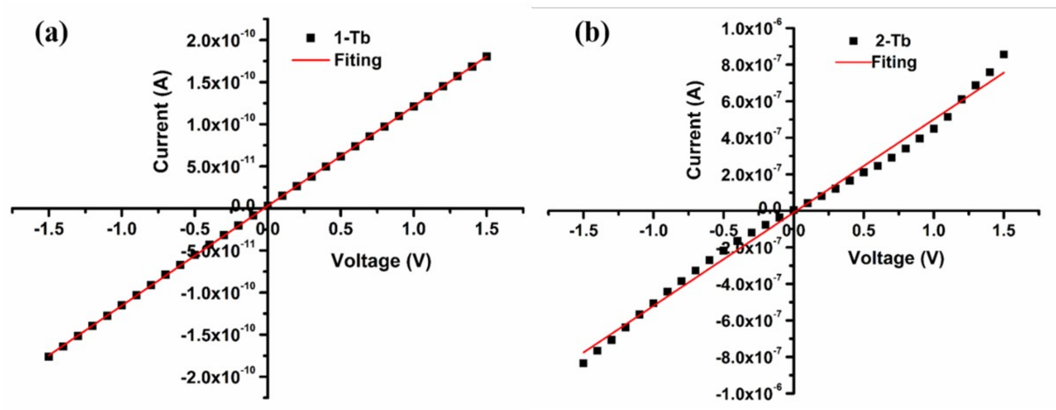

Figure S16. I-V curves of **1-Tb** (a) and **2-Tb** (b).

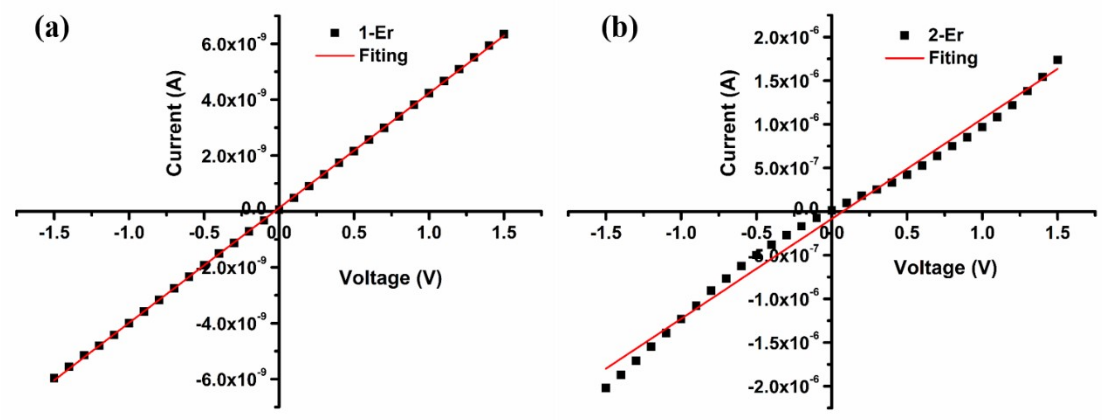

Figure S17. I-V curves of **1-Er** (a) and **2-Er** (b).

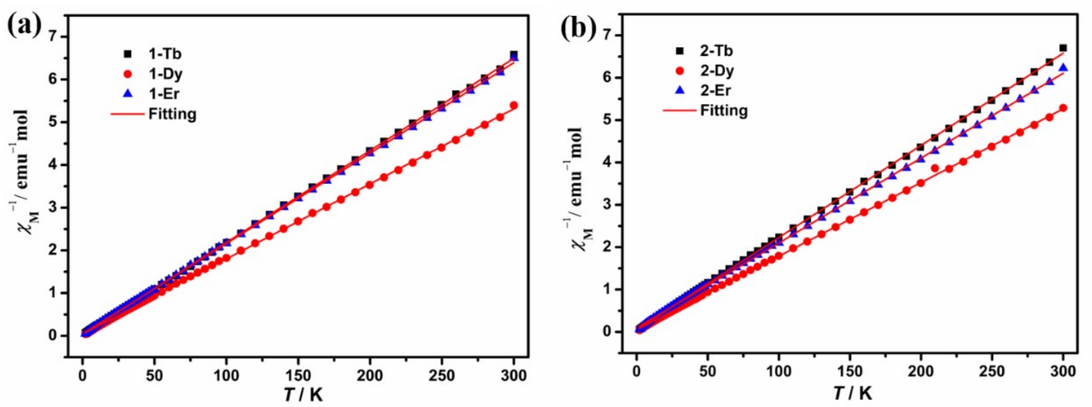

Figure S18. χ_M^{-1} *vs T* plots of MOFs **1-Ln** (a) and **2-Ln** (b). Red lines for the Curie-Weiss fitting.

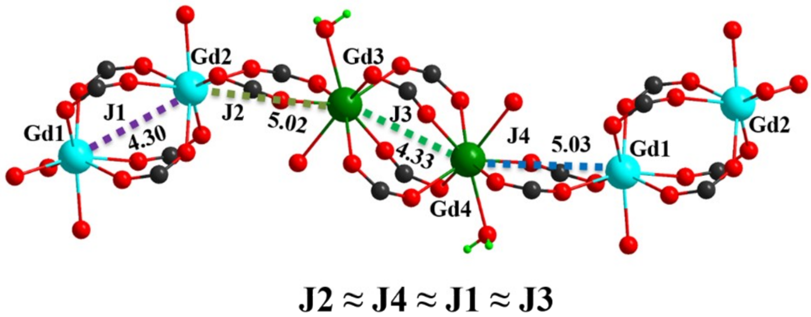

Figure S19. Four kinds of exchange interactions in one dimensional chain of **1-Gd**.

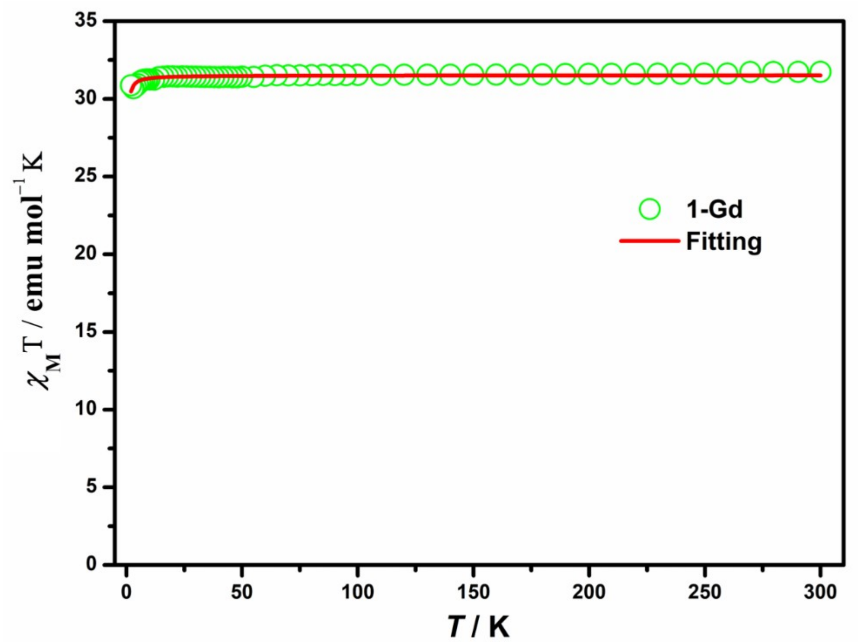

Figure S20. Plots of $\chi_M T$ *vs T* for **1-Gd**. The red line is the simulation of Gd_4 cluster only existing magnetic coupling.

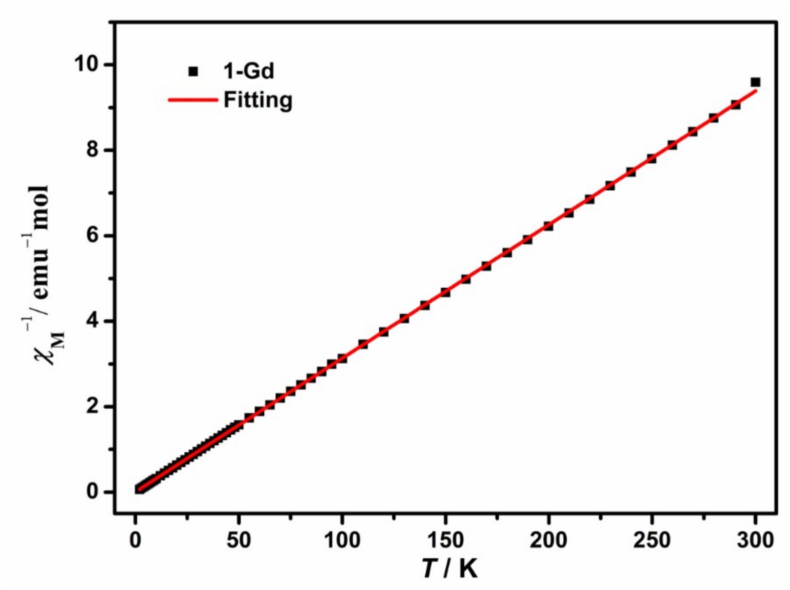

Figure S21. χ_M^{-1} *vs* T plots of **1-Gd**.

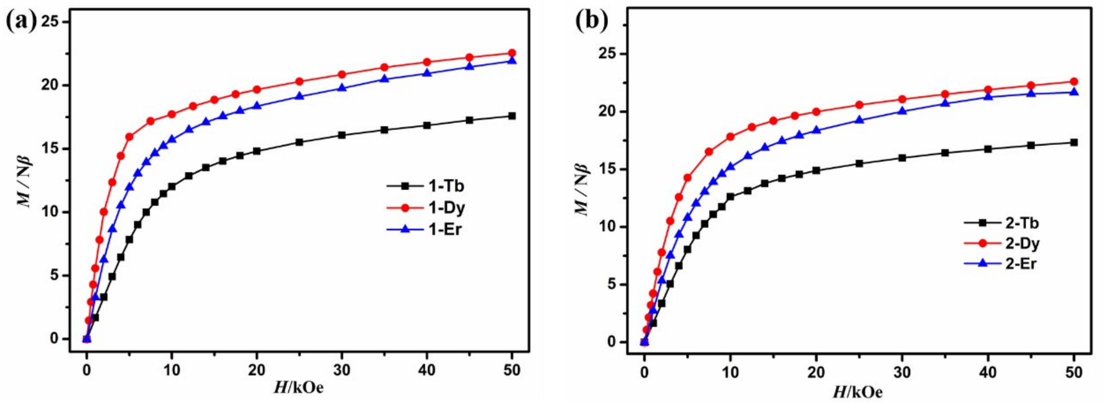

Figure S22. The *M* vs *H* curves of **1-Tb**, **1-Dy** and **1-Er** (a), **2-Tb**, and **2-Dy** and **2-Er** (b) at 2 K.

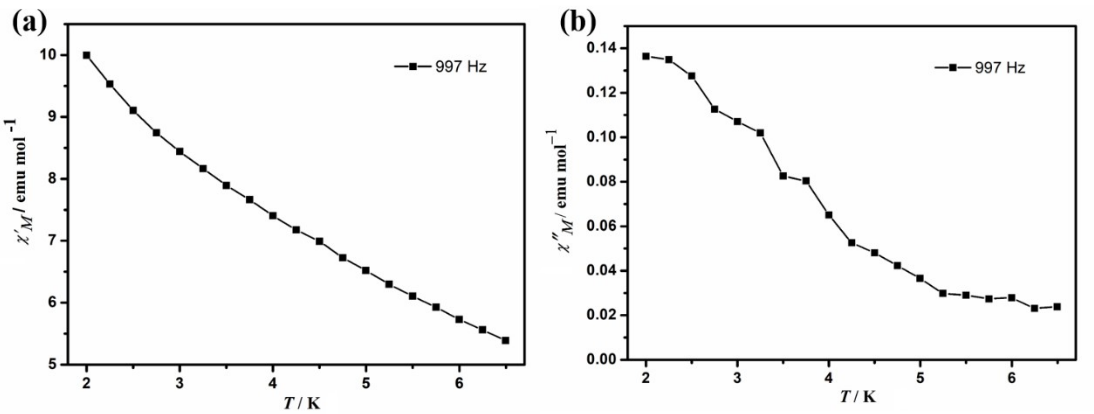

Figure S23. Temperature-dependent in-phase χ' (a) and out-of-phase χ'' (b) ac susceptibility signals for **1-Tb** at the frequency of 997 Hz under zero dc field.

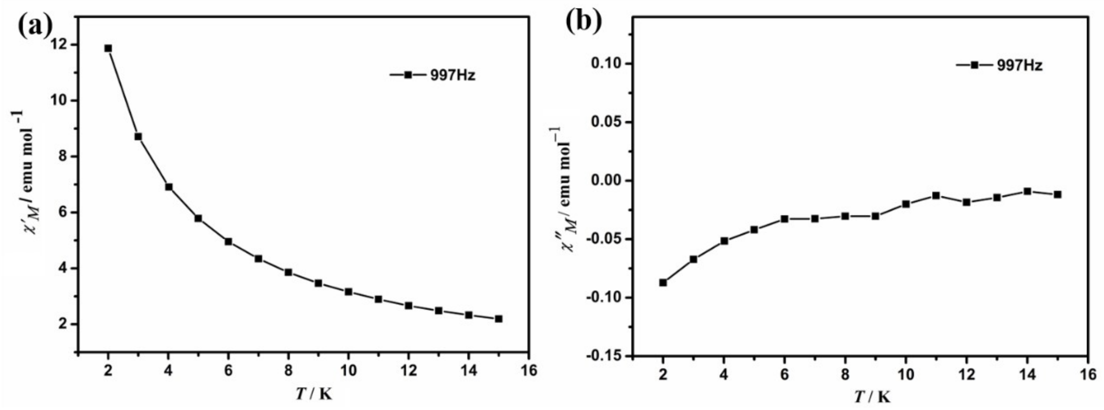

Figure S24. Temperature-dependent in-phase χ' (a) and out-of-phase χ'' (b) ac susceptibility signals for **2-Tb** at the frequency of 997 Hz under zero dc field.

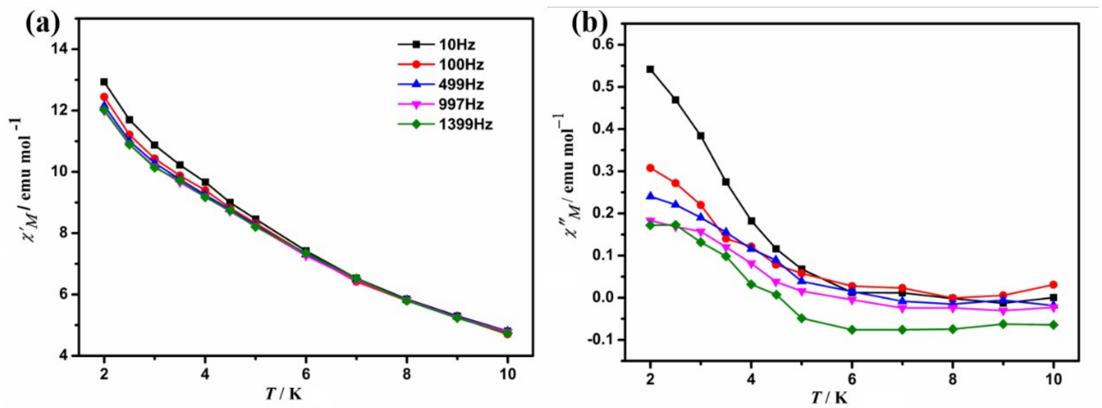

Figure S25. Temperature-dependent in-phase χ_M' (a) and out-of-phase χ_M'' (b) ac susceptibility signals for **1-Tb** under 2 kOe dc field.

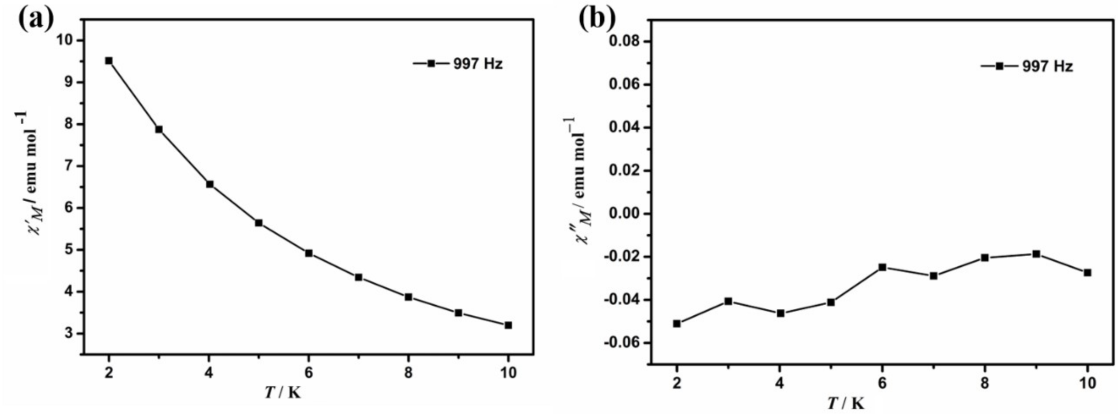

Figure S26. Temperature-dependent in-phase χ' (a) and out-of-phase χ'' (b) ac susceptibility signals for **2-Tb** at the frequency of 997 Hz under 2 kOe dc field.

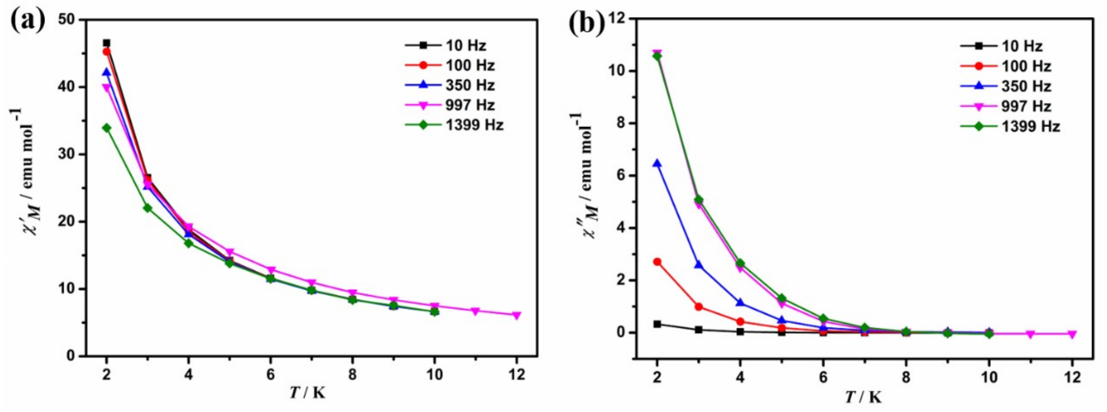

Figure S27. Temperature-dependent in-phase χ' (a) and out-of-phase χ'' (b) ac susceptibility signals for **1-Dy** under zero dc field.

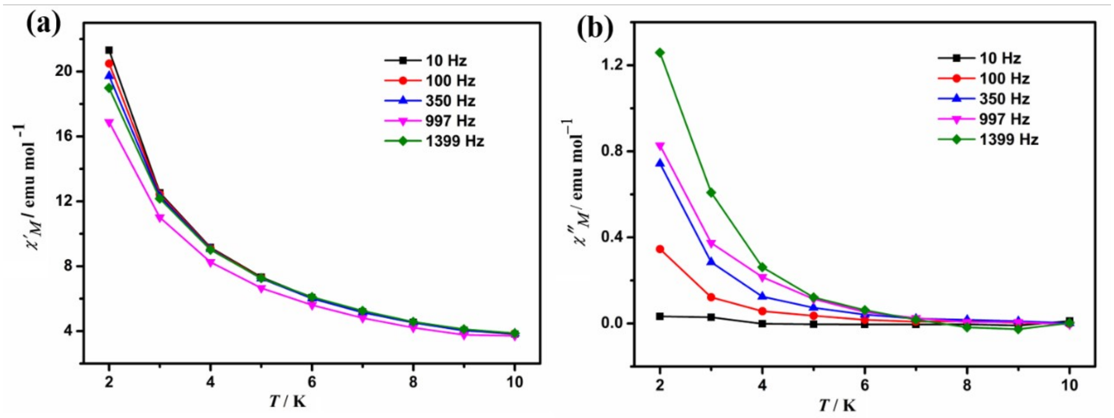

Figure S28. Temperature-dependent in-phase χ' (a) and out-of-phase χ'' (b) ac susceptibility signals for **2-Dy** under zero dc field.

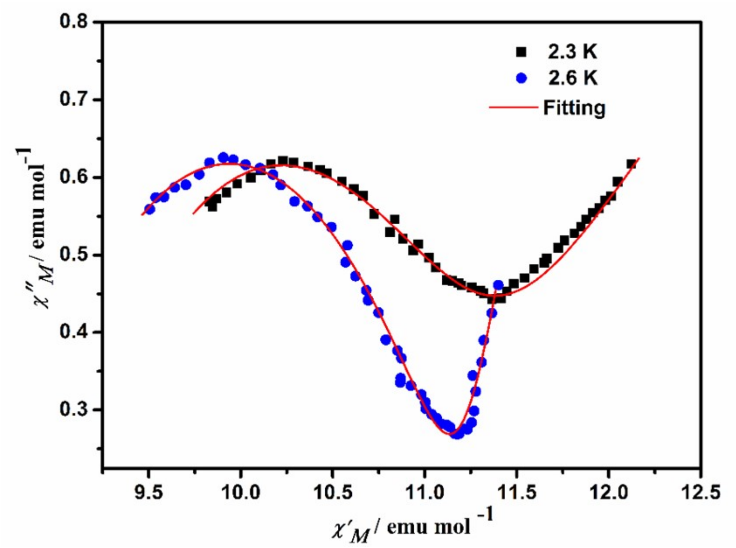

Figure S29. Cole-Cole plots for **2-Dy** under 1.5 kOe dc field. Solid lines represent the best fits to the one generalized Debye model.

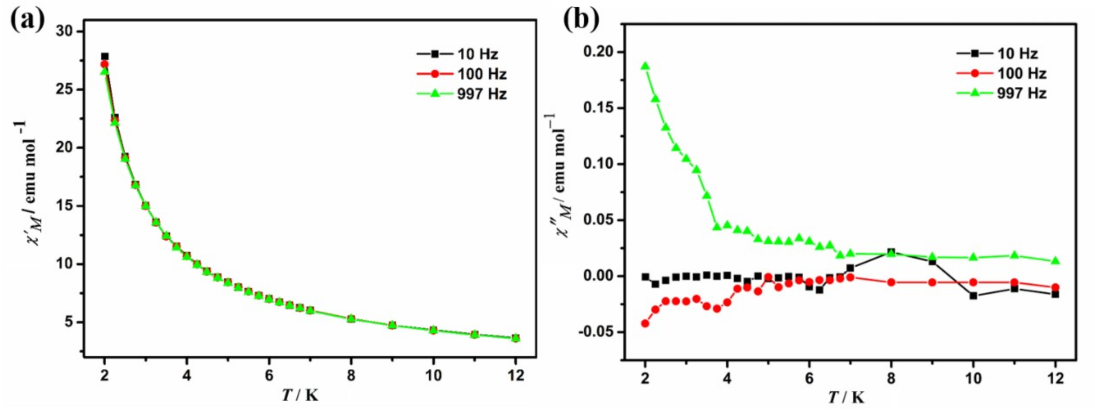

Figure S30. Temperature-dependent in-phase χ' (a) and out-of-phase χ'' (b) ac susceptibility signals for **1-Er** under zero dc field.

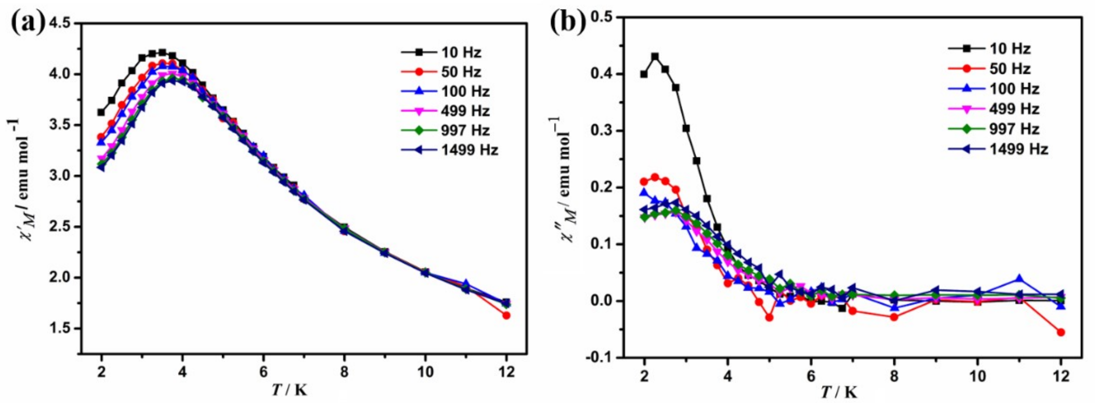

Figure S31. Temperature-dependent in-phase χ_M' (a) and out-of-phase χ_M'' (b) ac susceptibility signals for **1-Er** under 2 kOe dc field.

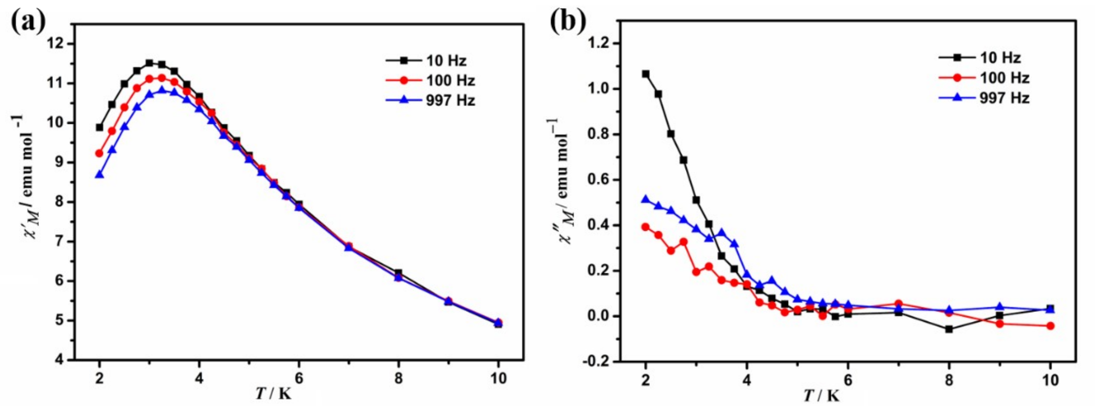

Figure S32. Temperature-dependent in-phase χ_M' (a) and out-of-phase χ_M'' (b) ac susceptibility signals for **2-Er** under 2 kOe dc field.

Table S1. Calculated values of elements with different oxidation degrees and test values of elemental analysis.

	I (%)				**II** (%)				Found (%)			
	C	N	H	S	C	N	H	S	C	N	H	S
2-Gd	20.80	1.60	1.28	22.19	18.74	1.50	1.15	19.99	19.73	1.78	1.45	20.97
2-Tb	20.78	1.62	1.27	22.18	18.72	1.46	1.14	19.96	20.73	1.81	1.78	23.14
2-Dy	20.66	1.61	1.26	22.04	18.63	1.45	1.14	19.87	20.43	1.52	1.62	21.78
2-Er	20.54	1.59	1.23	21.81	18.45	1.44	1.13	19.78	20.29	1.82	1.86	22.44

I: $\{[Ln_4(TTF\text{-}DC)_4(DMF)_4(H_2O)_2(TTF^{\bullet+}\text{-}DC)_2](I_3^-)_2\}_n$;

II: $\{[Ln_4(TTF\text{-}DC)_3(DMF)_4(H_2O)_2(TTF^{\bullet+}\text{-}DC)_3](I_3^-)_3\}_n$

Table S1. The weight loss value and TG analysis value of different oxidation degree between 100 and 240°C

	I (%)	**II** (%)	TG (%)
2-Gd	23.06	30.70	25.21
2-Tb	23.02	30.64	26.13
2-Dy	22.90	30.50	26.34
2-Er	22.67	30.21	23.21

I: $\{[Er_4(TTF\text{-}DC)_4(DMF)_4(H_2O)_2(TTF^{\bullet+}\text{-}DC)_2](I_3^-)_2\}_n$;

II: $\{[Er_4(TTF\text{-}DC)_3(DMF)_4(H_2O)_2(TTF^{\bullet+}\text{-}DC)_3](I_3^-)_3\}_n$

Table S3. Elemental analysis of **1-Gd** immersion time in cyclohexane solution of iodine (0.1 M).

	0 h (%)	24 h (%)	48 h (%)	72 h (%)
C	27.86	23.33	19.73	19.98
N	3.39	2.12	1.78	1.69
H	2.31	1.86	1.45	1.41

Table S4. Selected bond lengths (Å) and angles (º) for **1-Gd**

Gd01—O00T#1	2.492 (6)	Gd02—O3#4	2.378 (6)
Gd01—O00U	2.379 (6)	Gd02—O00Z#5	2.361 (6)
Gd01—O00W	2.338 (6)	Gd02—O010#6	2.410 (6)
Gd01—O00Y#2	2.429 (6)	Gd02—O011#6	2.478 (6)
Gd01—O01C#3	2.420 (6)	Gd02—O013#7	2.427 (6)
Gd01—O01D	2.344 (7)	Gd02—O018	2.338 (7)
Gd01—O01#1	2.510 (7)	Gd02—O01G	2.499 (7)
Gd01—O01L	2.531 (7)	Gd02—O01J	2.510 (7)
Gd03—O4	2.316 (6)	Gd04—O5	2.321 (6)
Gd03—O00X#6	2.411 (6)	Gd04—O012#6	2.400 (6)
Gd03—O014#8	2.397 (6)	Gd04—O01A	2.315 (6)
Gd03—O015#6	2.408 (6)	Gd04—O01B	2.270 (6)
Gd03—O016	2.287 (6)	Gd04—O01E#6	2.431 (7)
Gd03—O017	2.323 (6)	Gd04—O01F#1x	2.382 (6)
Gd03—O01Q	2.379 (8)	Gd04—O5	2.321 (6)
O00T#1—Gd01—O01#1	137.4 (2)	O3#4—Gd02—O010#6	80.5 (2)
O00U—Gd01—O00T#1	125.1 (2)	O00Z#5—Gd02—O3#4	71.1 (2)
O00W—Gd01—O00T#1	79.6 (2)	O010#6—Gd02—O011#6	73.5 (2)
O00Y#2—Gd01—O00T#1	73.8 (2)	O011#6—Gd02—O01G	136.8 (2)
O01C#3—Gd01—O00T#1	144.8 (2)	O013#7—Gd02—O011#6	145.5 (2)
O01D—Gd01—O00T#1	79.7 (2)	O018—Gd02—O3#4	146.3 (2)
O01#1—Gd01—O01L	124.9 (3)	O01G—Gd02—O01J	125.9 (3)
O4—Gd03—O00X#6	78.0 (2)	O2—Gd04—O012#6	73.3 (3)
O014#8—Gd03—O00X#6	147.1 (2)	O5—Gd04—O2	146.6 (3)
O015#6—Gd03—O00X#6	73.8 (2)	O012#6—Gd04—O01E#6	73.4 (2)
O016—Gd03—O4	158.9 (3)	O01A—Gd04—O2	79.4 (4)
O017—Gd03—O00X#6	124.1 (2)	O01B—Gd04—O2	80.2 (3)
O01Q—Gd03—O00X#6	73.1 (3)	O01F#1x—Gd04—O012#6	147.2 (3)

Symmetry codes: (#1) *x*, *y*, *z*+1; (#2) -*x*+1, -*y*+2, -*z*+3; (#3) -*x*+1/2, *y*+1/2, -*z*+3/2; (#4) -*x*+1, -*y*+1, -*z*; (#5) *x*, *y*-1, *z*-2; (#6) -*x*+1, -*y*+1, -*z*+1; (#7) -*x*+1/2, *y*-1/2, -*z*+1/2; (#8) -*x*+1/2, *y*-1/2, -*z*+3/2.

Table S5. Selected bond lengths (Å) and angles (º) for **1-Tb**

Tb1—O27$^{\#1}$	2.497 (6)	Tb2—O2	2.336 (7)
Tb1—O3$^{\#2}$	2.404 (6)	Tb2—O26$^{\#5}$	2.378 (6)
Tb1—O4	2.337 (7)	Tb2—O6$^{\#6}$	2.404 (6)
Tb1—O5	2.506 (7)	Tb2—O9$^{\#2}$	2.465 (6)
Tb1—O11	2.377 (6)	Tb2—O14	2.358 (6)
Tb1—O12	2.522 (7)	Tb2—O15	2.511 (7)
Tb1—O22$^{\#3}$	2.411 (6)	Tb2—O17	2.496 (7)
Tb1—O32$^{\#4}$	2.324 (6)	Tb2—O31$^{\#7}$	2.414 (6)
O28—Tb3$^{\#6}$	2.373 (6)	Tb4—O7	2.367 (8)
Tb3—O13$^{\#8}$	2.389 (6)	Tb4—O16$^{\#1}$	2.376 (7)
Tb3—O19	2.323 (7)	Tb4—O18$^{\#6}$	2.437 (7)
Tb3—O20	2.315 (6)	Tb4—O21$^{\#6}$	2.393 (6)
Tb3—O23	2.270 (7)	Tb4—O25$^{\#6}$	2.303 (6)
Tb3—O24	2.384 (6)	Tb4—O30	2.257 (7)
O1—Tb3	2.369 (8)	O29—Tb4	2.311 (7)
O27$^{\#1}$—Tb1—O5	137.3 (2)	O2—Tb2—O26$^{\#5}$	146.3 (2)
O3$^{\#2}$—Tb1—O27$^{\#1}$	73.3 (2)	O26$^{\#5}$—Tb2—O6$^{\#6}$	80.3 (2)
O4—Tb1—O27$^{\#1}$	79.7 (2)	O6$^{\#6}$—Tb2—O9$^{\#2}$	73.0 (2)
O5—Tb1—O12	125.6 (3)	O9$^{\#2}$—Tb2—O15	74.2 (2)
O11—Tb1—O27$^{\#1}$	124.9 (2)	O14—Tb2—O26$^{\#5}$	70.9 (2)
O22$^{\#3}$—Tb1—O27$^{\#1}$	144.9 (2)	O17—Tb2—O15	126.4 (2)
O32$^{\#4}$—Tb1—O27$^{\#1}$	80.1 (2)	O31$^{\#7}$—Tb2—O9$^{\#2}$	145.7 (2)
O1—Tb3—O28$^{\#6}$	73.0 (3)	O16$^{\#1}$—Tb4—O18$^{\#6}$	139.9 (2)
O28$^{\#6}$—Tb3—O13$^{\#8}$	147.0 (2)	O21$^{\#6}$—Tb4—O18$^{\#6}$	72.7 (2)
O19—Tb3—O1	78.9 (3)	O25$^{\#6}$—Tb4—O29	78.6 (3)
O20—Tb3—O1	147.5 (3)	O30—Tb4—O29	118.7 (3)
O23—Tb3—O1	79.8 (3)	O7—Tb4—O16$^{\#1}$	78.1 (3)
O24—Tb3—O13$^{\#8}$	139.5 (2)	O29—Tb4—O7	147.1 (3)

Symmetry codes: (#1) -x+1, -y+2, -z+1; (#2) -x+1, -y+2, -z; (#3) -x+1/2, y+1/2, -z+1/2; (#4) x, y+1, z-2; (#5) x, y, z-1; (#6) -x+1, -y+1, -z+2; (#7) -x+1/2, y+1/2, -z+3/2; (#8) -x+1/2, y-1/2, -z+1/2.

Table S6. Selected bond lengths (Å) and angles (º) for **1-Dy**

Dy01—O00T	2.286 (5)	Dy02—O00U$^{\#2}$	2.350 (5)
Dy01—O00$^{\#5}$	2.342 (5)	Dy02—O00Y	2.380 (5)
Dy01—O00W$^{\#1}$	2.388 (5)	Dy02—O011	2.431 (5)
Dy01—O010$^{\#2}$	2.453 (5)	Dy02—O016$^{\#1}$	2.302 (5)
Dy01—O01C$^{\#3}$	2.379 (5)	Dy02—O019	2.291 (5)
Dy01—O01E	2.292 (5)	Dy02—O01B$^{\#4}$	2.366 (5)
Dy01—O01J	2.483 (6)	Dy02—O01H	2.474 (5)
Dy01—O01L	2.480 (6)	Dy02—O01$^{\#1}$	2.468 (6)
Dy03—O3	2.330 (6)	Dy04—O5	2.356 (5)
Dy03—O4	2.273 (5)	Dy04—O00X$^{\#6}$	2.248 (5)
Dy03—O00Z	2.306 (5)	Dy04—O012	2.301 (5)
Dy03—O013	2.236 (5)	Dy04—O015	2.375 (5)
Dy03—O018	2.391 (5)	Dy04—O01D$^{\#7}$	2.358 (5)
Dy03—O01F$^{\#5}$	2.345 (5)	Dy04—O01M	2.339 (6)
O2—Dy03	2.354 (5)	O1—Dy04	2.276 (5)
O00T—Dy01—O00$^{\#5}$	72.76 (19)	O00U$^{\#2}$—Dy02—O00Y	79.78 (17)
O00#5—Dy01—O00W$^{\#1}$	79.92 (18)	O00Y—Dy02—O011	72.72 (18)
O00W$^{\#1}$—Dy01—O010$^{\#2}$	72.89 (17)	O011—Dy02—O01H	136.85 (18)
O010$^{\#2}$—Dy01—O01J	137.01 (18)	O016$^{\#1}$—Dy02—O00U$^{\#2}$	71.72 (18)
O01C$^{\#3}$—Dy01—O00W$^{\#1}$	141.46 (18)	O019—Dy02—O00U$^{\#2}$	145.8 (2)
O01C$^{\#3}$—Dy01—O010$^{\#2}$	145.21 (18)	O01B$^{\#4}$—Dy02—O00Y	141.15 (18)
O01E—Dy01—O00$^{\#5}$	144.4 (2)	O01$^{\#1}$—Dy02—O01H	126.7 (2)
O2—Dy03—O018	72.87 (19)	O1—Dy04—O5	79.19 (18)
O3—Dy03—O2	73.3 (2)	O5—Dy04—O015	73.20 (19)
O4—Dy03—O2	79.17 (19)	O00X$^{\#6}$—Dy04—O1	159.5 (2)
O00Z—Dy03—O2	124.90 (19)	O012—Dy04—O5	123.55 (19)
O013—Dy03—O2	98.72 (18)	O01D$^{\#7}$—Dy04—O015	137.88 (18)
O01F$^{\#5}$—Dy03—O2	148.30 (19)	O01M—Dy04—O5	73.7 (2)

Symmetry codes: (#1) -*x*+1, -*y*, -*z*+2; (#2) *x*, *y*, *z*+1; (#3) -*x*+1/2, *y*-1/2, -*z*+1/2; (#4) *x*+1/2, -*y*+1/2, *z*+1/2; (#5) *x*-1/2, -*y*+1/2, *z*-1/2; (#6) -*x*+1, -*y*+1, -*z*; (#7) *x*+1/2, -*y*+1/2, *z*-1/2; (#8) -*x*+1, -*y*, -*z*+1.

Table S7. Selected bond lengths (Å) and angles (º) for **1-Er**

Er01—O8	2.256 (6)	Er02—O23	2.277 (6)
Er01—O5	2.324 (5)	Er02—O21	2.245 (6)
Er01—O1	2.360 (6)	Er02—O19	2.331 (6)
Er01—O10	2.426 (6)	Er02—O27	2.369 (6)
Er01—O31$^{\#1}$	2.260 (6)	Er02—O14$^{\#3}$	2.202 (6)
Er01—O16$^{\#2}$	2.350 (6)	Er02—O28$^{\#4}$	2.326 (6)
Er01—O7	2.471 (7)	Er02—O18	2.309 (7)
Er01—O4	2.470 (7)	Er02—O23	2.277 (6)
Er03—O11	2.326 (5)	Er04—O20	2.278 (6)
Er03—O2	2.277 (6)	Er04—O24	2.334 (6)
Er03—O9	2.352 (5)	Er04—O17$^{\#7}$	2.220 (6)
Er03—O13$^{\#5}$	2.345 (6)	Er04—O26	2.243 (6)
Er03—O29$^{\#6}$	2.256 (6)	Er04—O30$^{\#8}$	2.336 (5)
Er03—O6	2.403 (6)	Er04—O25	2.316 (7)
Er03—O12	2.451 (6)	Er04—O22	2.352 (6)
O8—Er01—O5	73.5 (2)	O23—Er02—O19	124.6 (2)
O5—Er01—O1	79.3 (2)	O21—Er02—O23	79.0 (2)
O1—Er01—O10	72.8 (2)	O19—Er02—O27	72.5 (2)
O10—Er01—O7	74.0 (2)	O14$^{\#3}$—Er02—O23	116.5 (2)
O31$^{\#1}$—Er01—O5	144.0 (2)	O28$^{\#4}$—Er02—O19	149.1 (2)
O16$^{\#2}$—Er01—O1	141.3 (2)	O18—Er02—O19	73.4 (3)
O4—Er01—O7	125.6 (3)	O23—Er02—O19	124.6 (2)
O11—Er03—O9	79.1 (2)	O20—Er04—O24	123.2 (2)
O2—Er03—O11	72.1 (2)	O24—Er04—O30$^{\#8}$	149.6 (2)
O9—Er03—O6	72.7 (2)	O17$^{\#7}$—Er04—O20	117.9 (2)
O13$^{\#5}$—Er03—O9	141.3 (2)	O26—Er04—O20	78.5 (2)
O29$^{\#6}$—Er03—O11	145.8 (2)	O30$^{\#8}$—Er04—O22	137.4 (2)
O6—Er03—O3	74.2 (2)	O25—Er04—O24	73.8 (3)

Symmetry codes: (#1) -*x*+1, -*y*+1, -*z*+1; (#2) -*x*+3/2, *y*+1/2, -*z*+3/2; (#3) *x*, *y*, *z*-1; (#4) *x*+1/2, -*y*+1/2, *z*+1/2; (#5) *x*-1/2, -*y*+1/2, *z*-1/2; (#6) *x*, *y*, *z*+1; (#7) -*x*+1, -*y*, -*z*+1; (#8) -*x*+1/2, *y*-1/2.

Table S8. SHAPE analyses of the Ln^{III} ions in **1-Ln**

Complex	Metal Ions	Label	Shape	Symmetry	Distortion(τ)
1-Gd	Gd1/Gd2	HP-7	D_{7h}	Heptagon	31.699/31.971
		HPY-7	C_{6v}	Hexagonal pyramid	21.063/21.321
		PBPY-7	D_{5h}	Pentagonal bipyramid	5.732/5.326
		COC-7	C_{3v}	Capped octahedron	0.931/0.988
		CTPR-7	$\boldsymbol{C_{2v}}$	**Capped trigonal prism**	**0.844/0.838**
		JPBPY-7	D_{5h}	Johnson pentagonal bipyramid J13	8.749/8.315
		JETPY-7	C_{3v}	Johnson elongated triangular pyramid J7	18.506/18.599
	Gd3/Gd4	OP-8	D_{8h}	Octagon	28.473/28.635
		HPY-8	C_{7v}	Heptagonal pyramid	24.528/24.548
		HBPY-8	D_{6h}	Hexagonal bipyramid	16.320/15.916
		CU-8	O_h	Cube	10.404/9.978
		SAPR-8	D_{4d}	Square antiprism	1.162/1.177
		TDD-8	D_{2d}	Triangular dodecahedron	1.355/1.206
		JGBF-8	D_{2d}	Johnson gyrobifastigium J26	14.470/14.488
		JETBPY-8	D_{3h}	Johnson elongated triangular bipyramid J14	28.529/28.381
		JBTPR-8	C_{2v}	Biaugmented trigonal prism J50	1.171/1.297
		BTPR-8	$\boldsymbol{C_{2v}}$	**Biaugmented trigonal prism**	**0.695/0.812**
		JSD-8	D_{2d}	Snub diphenoid J84	3.172/3.204
		TT-8	T_d	Triakis tetrahedron	10.914/10.538
		ETBPY-8	D_{3h}	Elongated trigonal bipyramid	24.789/24.640
1-Tb	Tb1/Tb2	HP-7	D_{7h}	Heptagon	31.684/31.697
		HPY-7	C_{6v}	Hexagonal pyramid	20.981/21.341
		PBPY-7	D_{5h}	Pentagonal bipyramid	5.806/5.327
		COC-7	C_{3v}	Capped octahedron	0.894/1.018
		CTPR-7	$\boldsymbol{C_{2v}}$	**Capped trigonal prism**	**0.855/0.871**
		JPBPY-7	D_{5h}	Johnson pentagonal bipyramid J13	8.897/8.225
		JETPY-7	C_{3v}	Johnson elongated triangular pyramid J7	18.493/18.435
	Tb3/Tb4	OP-8	D_{8h}	Octagon	28.287/28.626
		HPY-8	C_{7v}	Heptagonal pyramid	24.480/24.472
		HBPY-8	D_{6h}	Hexagonal bipyramid	16.420/15.904
		CU-8	O_h	Cube	10.539/10.118
		SAPR-8	D_{4d}	Square antiprism	1.149/1.154
		TDD-8	D_{2d}	Triangular dodecahedron	1.386/1.279
		JGBF-8	D_{2d}	Johnson gyrobifastigium J26	14.326/14.315
		JETBPY-8	D_{3h}	Johnson elongated triangular bipyramid J14	28.550/28.445
		JBTPR-8	C_{2v}	Biaugmented trigonal prism	1.187/1.268

				J50	
		BTPR-8	$\boldsymbol{C_{2v}}$	**Biaugmented trigonal prism**	**0.735/0.829**
		JSD-8	D_{2d}	Snub diphenoid J84	3.114/3.243
		TT-8	T_d	Triakis tetrahedron	11.005/10.659
		ETBPY-8	D_{3h}	Elongated trigonal bipyramid	24.567/24.608
1-Dy	Dy1/Dy2	HP-7	D_{7h}	Heptagon	32.246/32.053
		HPY-7	C_{6v}	Hexagonal pyramid	21.565/21.247
		PBPY-7	D_{5h}	Pentagonal bipyramid	5.196/5.713
		COC-7	C_{3v}	Capped octahedron	0.917/0.831
		CTPR-7	$\boldsymbol{C_{2v}}$	**Capped trigonal prism**	**0.848/0.811**
		JPBPY-7	D_{5h}	Johnson pentagonal bipyramid J13	8.176/8.741
		JETPY-7	C_{3v}	Johnson elongated triangular pyramid J7	18.937/18.730
	Dy3/Dy4	OP-8	D_{8h}	Octagon	28.591/28.546
		HPY-8	C_{7v}	Heptagonal pyramid	24.327/24.312
		HBPY-8	D_{6h}	Hexagonal bipyramid	16.303/15.956
		CU-8	O_h	Cube	10.491/10.206
		SAPR-8	D_{4d}	Square antiprism	1.167/1.160
		TDD-8	D_{2d}	Triangular dodecahedron	1.384/1.276
		JGBF-8	D_{2d}	Johnson gyrobifastigium J26	14.380/14.402
		JETBPY-8	D_{3h}	Johnson elongated triangular bipyramid J14	28.634/28.401
		JBTPR-8	C_{2v}	Biaugmented trigonal prism J50	1.160/1.222
		BTPR-8	$\boldsymbol{C_{2v}}$	**Biaugmented trigonal prism**	**0.738/0.817**
		JSD-8	D_{2d}	Snub diphenoid J84	3.146/3.141
		TT-8	T_d	Triakis tetrahedron	10.966/10.712
		ETBPY-8	D_{3h}	Elongated trigonal bipyramid	24.675/24.667
1-Er	Er1/Er2	HP-7	D_{7h}	Heptagon	32.380/31.697
		HPY-7	C_{6v}	Hexagonal pyramid	21.526/21.341
		PBPY-7	D_{5h}	Pentagonal bipyramid	5.710/5.327
		COC-7	C_{3v}	Capped octahedron	0.743/1.018
		CTPR-7	$\boldsymbol{C_{2v}}$	**Capped trigonal prism**	0.863/ 0.871
		JPBPY-7	D_{5h}	Johnson pentagonal bipyramid J13	8.674/8.225
		JETPY-7	C_{3v}	Johnson elongated triangular pyramid J7	18.809/18.435
	Er3/Er4	OP-8	D_{8h}	Octagon	28.803/28.812
		HPY-8	C_{7v}	Heptagonal pyramid	24.312/24.278
		HBPY-8	D_{6h}	Hexagonal bipyramid	16.201/15.887
		CU-8	O_h	Cube	10.520/10.178
		SAPR-8	D_{4d}	Square antiprism	1.237/1.203
		TDD-8	D_{2d}	Triangular dodecahedron	1.422/1.276

		JGBF-8	D_{2d}	Johnson gyrobifastigium J26	14.410/14.395
		JETBPY-8	D_{3h}	Johnson elongated triangular bipyramid J14	28.700/28.530
		JBTPR-8	C_{2v}	Biaugmented trigonal prism J50	1.073/1.165
		BTPR-8	$\boldsymbol{C_{2v}}$	**Biaugmented trigonal prism**	**0.724/0.823**
		JSD-8	D_{2d}	Snub diphenoid J84	3.090/3.103
		TT-8	T_d	Triakis tetrahedron	10.944/10.660
		ETBPY-8	D_{3h}	Elongated trigonal bipyramid	24.935/24.870

Table S9. The fitting parameters α and τ values for **1-Dy** by using CC-FIT software.

T	α_1	τ_1	α_2	τ_2
2.0 K	0.52	0.42×10^{-4}	0.24	0.39
2.5 K	0.52	0.49×10^{-4}	0.30	0.47
3 K	0.46	0.72×10^{-4}	0.39	0.62

Table S10. The fitting parameters α and τ values for **2-Dy** by using CC-FIT software.

T	α_1	τ_1	α_2	τ_2
2.3 K	0.43	0.26×10^{-3}	0.65	0.20
2.6 K	0.44	0.32×10^{-3}	0.32	0.64